JOURNAL OF GEOPHYSICAL RESEARCH, VOL. 117, D20201, doi:10.1029/2012JD017950, 2012

Climate impacts of ice nucleation

A. Gettelman,[1,2] X. Liu,[3] D. Barahona,[4,5] U. Lohmann,[2] and C. Chen[1]

Received 16 April 2012; revised 11 September 2012; accepted 16 September 2012; published 19 October 2012.

[1] Several different ice nucleation parameterizations in two different General Circulation Models (GCMs) are used to understand the effects of ice nucleation on the mean climate state, and the Aerosol Indirect Effects (AIE) of cirrus clouds on climate. Simulations have a range of ice microphysical states that are consistent with the spread of observations, but many simulations have higher present-day ice crystal number concentrations than in-situ observations. These different states result from different parameterizations of ice cloud nucleation processes, and feature different balances of homogeneous and heterogeneous nucleation. Black carbon aerosols have a small (-0.06 Wm^{-2}) and not statistically significant AIE when included as ice nuclei, for nucleation efficiencies within the range of laboratory measurements. Indirect effects of anthropogenic aerosols on cirrus clouds occur as a consequence of increasing anthropogenic sulfur emissions with different mechanisms important in different models. In one model this is due to increases in homogeneous nucleation fraction, and in the other due to increases in heterogeneous nucleation with coated dust. The magnitude of the effect is the same however. The resulting ice AIE does not seem strongly dependent on the balance between homogeneous and heterogeneous ice nucleation. Regional effects can reach several Wm^{-2}. Indirect effects are slightly larger for those states with less homogeneous nucleation and lower ice number concentration in the base state. The total ice AIE is estimated at 0.27 ± 0.10 Wm^{-2} (1σ uncertainty). This represents a 20% offset of the simulated total shortwave AIE for ice and liquid clouds of -1.6 Wm^{-2}.

Citation: Gettelman, A., X. Liu, D. Barahona, U. Lohmann, and C. Chen (2012), Climate impacts of ice nucleation, *J. Geophys. Res.*, *117*, D20201, doi:10.1029/2012JD017950.

1. Introduction

[2] Ice clouds play an important role in the climate system. Ice clouds reflect solar radiation back to space, cooling the planet. However, ice clouds, being cold, radiate much less long wave radiation to space than low clouds or the surface, thus also heating the planet. The balance of these two processes determines the net ice cloud radiative forcing, which is finely balanced between warming and cooling, with warming thought to be slightly larger.

[3] Changes to ice cloud microphysics might alter this balance. Since ice clouds are nucleated by aerosol particles, changes to the aerosol composition in ice cloud regions may alter cloud microphysics and ice cloud radiative forcing. These are commonly called 'Aerosol Indirect Effects', or AIE [*Twomey*, 1977], reviewed by *Lohmann and Feichter* [2005]. While the AIE of liquid clouds is predominately a short wave cooling by reflection of solar radiation off of brighter cloud tops, cold ice clouds also have longwave effects, and complex interactions between aerosol and crystal number [*Kärcher et al.*, 2006] that can lead to warming or cooling. There remain major uncertainties in ice nucleation processes [*DeMott et al.*, 2011], and while several representations of ice nucleation now exist [*Liu and Penner*, 2005; *Kärcher et al.*, 2006; *Barahona and Nenes*, 2009], and global models are incorporating them with comprehensive aerosol schemes [*Lohmann and Hoose*, 2009; *Gettelman et al.*, 2010] there are limited estimates of the global impact of ice nucleation on climate. *Penner et al.* [2009] performed estimates using off-line radiative transfer calculations and found no net effect from sulfate, but a cooling effect from Black Carbon soot (see below). *Liu et al.* [2009] estimated the ice AIE using the Community Atmosphere Model (CAM) version 3 of 0.5–0.7 Wm^{-2} and lower stratospheric water vapor increases of 0.3 ppmv.

[4] There are major uncertainties in the types of ice nuclei and the mechanisms by which ice clouds form that complicate assessment of ice indirect effects. The role of different aerosol types in nucleating ice at different threshold humidities is uncertain [*DeMott et al.*, 2011]. Attempts at estimating indirect effects need to account for these uncertainties, which are driven by wide variations in ice microphysical measurements [*Krämer et al.*, 2009].

[1]National Center for Atmospheric Research, Boulder, Colorado, USA.
[2]Institute for Atmospheric and Climate Science, ETH Zurich, Zurich, Switzerland.
[3]Pacific Northwest National Laboratory, Richland, Washington, USA.
[4]NASA Goddard Space Flight Center, Greenbelt, Maryland, USA.
[5]I. M. Systems Group, Rockville, Maryland, USA.

Corresponding author: A. Gettelman, National Center for Atmospheric Research, 1850 Table Mesa Dr., Boulder, CO 80305, USA. (andrew@ucar.edu)

0148-0227/12/2012JD017950

Table 1. Description of Simulation Pairs Used in This Study[a]

Name	Ice Nucleation	Description
CAM5-LP	*Liu et al.* [2007]	Base CAM5 (LP2007 Ice Nucleation)
CAM5-FixedIN	*Cooper* [1986]	Ice Nuclei a function of temperature
CAM5-LP-BC-0.1%	*Liu et al.* [2007]	Base + 0.1% BC included as heterogeneous IN
CAM5-LP-BC-2%	*Liu et al.* [2007]	Base + 2% BC included as heterogeneous IN
CAM5-LP-BC-100%	*Liu et al.* [2007]	Base + all BC included as heterogeneous IN
CAM5-BN	*Barahona and Nenes* [2009]	BN2009 with $D_{SO4} > 0.05$ μm
CAM5-BN-Low	*Barahona and Nenes* [2009]	BN2009 with $D_{SO4} > 0.1$ μm
CAM5-LP-Low	*Liu et al.* [2007]	Base with 40% less ice mass
CAM5-LP-W10	*Liu et al.* [2007]	CAM5-LP2007 with sub-grid W × 10
CAM5-LP-FixedDN	*Liu et al.* [2007]	Base code with fixed drop number
CAM5-BN-FixedDN	*Barahona and Nenes* [2009]	BN2009 code with fixed drop number
ECHAM5-FixedDN	*Kärcher and Lohmann* [2002]	Fixed drop number

[a]Each simulation pair is the difference between aerosol emissions from the year 2000 and 1850, with annually repeating climatological SST and greenhouse gases. For CAM5-FixedIN, *Cooper* [1986] specifies IN = 209 L^{-1} for T < −30°C.

[5] One of the major uncertainties with respect to ice nucleation is understanding the importance of natural and anthropogenic Black Carbon (BC, also known as soot). Process [*Kärcher and Lohmann*, 2003; *Kärcher et al.*, 2007] and global [*Lohmann et al.*, 2004; *Hendricks et al.*, 2005; *Penner et al.*, 2009; *Liu et al.*, 2009; *Hendricks et al.*, 2011] model studies found significant impacts of BC on cirrus clouds if they are assumed to be efficient ice nuclei [e.g., *Penner et al.*, 2009]. *Barahona et al.* [2010] compared several descriptions of heterogeneous ice nucleation within the same parameterization framework and found that a soot ice activation fraction of 1% would be enough to significantly impact the global distribution of ice crystal concentration at cirrus levels.

[6] The assumption that BC can heterogeneously nucleate ice crystals at humidities below the homogeneous nucleation limit (RH_i of 130–150% depending on temperature) is not certain. Cloud chamber measurements by *Möhler et al.* [2005] found that 0.1–0.3% of uncoated BC particles freeze at supersaturations from 1.1–1.3 (110% < RH_i < 130%). But *DeMott et al.* [2009] could not find heterogeneous freezing of biomass burning aerosols in controlled burning laboratory experiments. Neither did *Friedman et al.* [2011] for controlled experiments with coated soot at pure ice formation temperatures (−35°C). However, assuming that BC aerosols are efficient ice nuclei at low supersaturations (RH_i = 130%), *Penner et al.* [2009] find using off-line calculations significant and large impacts of anthropogenic BC on cirrus clouds, with radiative forcing of up to −0.4 Wm^{-2} from the indirect effects of BC, but with a high BC mass loading of 3× observations [*Wang et al.*, 2009]. *Crawford et al.* [2011] found that between 0.1–1% of soot particles with low organic carbon content would nucleate ice at T ∼ 220 K in the deposition mode. *Barahona* [2011] showed that this is consistent with a soot ice nucleation fraction increasing from about 0.01% to 10% for RH_i ∼135% to RH_i ∼170%, respectively, and with the soot IN activity increasing for decreasing temperature.

[7] This study will investigate (a) the different climate states of humidity and clouds simulated by different ice nucleation schemes, (b) anthropogenic effects on ice clouds and (c) the role of BC in altering ice cloud radiative forcing.

[8] We will investigate these properties using two different advanced General Circulation Models (GCMs), the National Center for Atmospheric Research (NCAR) Community Atmosphere Model version 5 (CAM5), and the European Center Hamburg (ECHAM) model version 5 with the Hamburg Aerosol Model (ECHAM5-HAM). We will use 3 different ice nucleation parameterizations in several different configurations, and a version of CAM5 with no ice indirect effects, to examine the impact of ice nucleating aerosols on climate.

[9] Models and experiment methodology (Section 2) are defined below. Baseline results with present-day emissions, and the impact of BC in present day are discussed in Section 3. Ice AIE estimates are presented in Section 4. The paper finishes with a discussion (Section 5) and conclusions in Section 6.

2. Models and Experiments

2.1. CAM5 Description

[10] The primary model used in this study is CAM5 from the National Center for Atmospheric Research (NCAR). CAM5 includes an advanced physical parameterization suite [*Gettelman et al.*, 2010; *Neale et al.*, 2010] that is well suited for understanding ice nucleation. CAM5 has a 2-moment cloud microphysics scheme [*Morrison et al.*, 2005; *Gettelman et al.*, 2008], coupled to a Modal Aerosol Model with 3 modes [*Liu et al.*, 2012a]. The model allows ice supersaturation, and links ice cloud particles consistently to aerosols through ice nucleation (see below). Aerosols in CAM5 do not interact with convective cloud drops and ice crystals. Convective detrainment of ice into anvils is based on temperature (all ice below −30°C) and a prescribed mean radius of 25 μm. CAM5 has a consistent treatment of the radiative effects of ice clouds and snow (see *Gettelman et al.* [2010] for details).

2.1.1. CAM Ice Nucleation

[11] CAM5 simulates ice nucleation in mixed phase and cirrus (pure ice) clouds. Ice nucleation for cirrus (pure ice) clouds (T< −35°C) is parameterized following *Liu and Penner* [2005] and *Liu et al.* [2007], hereafter LP2007, implemented as described by *Gettelman et al.* [2010]. This simulation we term CAM5-LP (Table 1). The parameterization features competition between heterogeneous nucleation (immersion freezing) on dust with homogeneous nucleation on sulfate. Unlike LP2007, nucleation of BC is not active in the standard CAM5 [*Gettelman et al.*, 2010]. CAM5 homogeneous ice nucleation uses Aiken mode sulfate aerosol particles larger than 0.1 μm diameter. CAM5 uses dust in

the coarse mode as potential heterogeneous ice nuclei (IN) [*Gettelman et al.*, 2010], consistent with classical theory and IN observations [*Pruppacher and Klett*, 1997]. We also test adding BC as IN with the same properties of dust as in *Liu et al.* [2007] or *Penner et al.* [2009], with an efficiency of 0.1%, 2% or 100% (CAM5-LP-BC cases in Table 1). CAM5 in the mixed phase regime ($-40°C < T < -3°C$), features empirical formulations for ice nucleation for deposition and condensation freezing [*Meyers et al.*, 1992], immersion freezing [*Bigg*, 1953], prescribed without explicit dependance on aerosols, and contact freezing on dust [*Young*, 1974].

[12] Since the grid-scale vertical velocity is the net of larger small scale motions, CAM5 ice nucleation is driven by a sub-grid scale vertical velocity. The velocity is derived from the Turbulent Kinetic Energy (TKE) scheme [*Park and Bretherton*, 2009]. In the upper troposphere, this velocity is typically 5–10 cm s^{-1}, smaller near the tropopause, and larger near deep convective clouds. In general this velocity is lower than that seen in limited observations from aircraft in cirrus anvils [*Jensen et al.*, 2009] of 30–50 cm s^{-1}, and an order of magnitude smaller than convective motions, but is reflective of mean motions in large scale cirrus clouds and radiative uplift [*Corti et al.*, 2005]. We have performed a sensitivity experiment with the sub-grid vertical velocity for ice nucleation increased by a factor of 10 (CAM5-LP-W10), where the mean is 30–80 cm s^{-1} to test potential impacts of the specification of vertical motion on the results.

2.1.2. Alternative Ice Nucleation

[13] For comparison, we have also implemented an alternative cirrus ice nucleation scheme to the base version of CAM5. This is the parameterization of *Barahona and Nenes* [2009], hereafter BN2009 (CAM5-BN). Similar to LP2007, it estimates the maximum supersaturation achieved in a rising air parcel and an aerosol spectrum to estimate ice crystal concentrations. However, whereas LP2007 is derived from fits to the numerical solution of the parcel model equations, BN2009 is derived from an approximation to their analytical solution. Using offline calculations *Barahona and Nenes* [2008] have shown that for similar values of the ice deposition coefficient and pure homogeneous freezing, ice number concentration (N_i) from BN2009 and LP2007 agree within a factor of 2 for T > 200 K. However, the two parameterizations largely differ in their treatment of heterogeneous ice nucleation and the competition between homogeneous and heterogeneous freezing. LP2007 used a combination of classical nucleation theory and empirical formulations to describe the freezing of dust and soot IN. BN2009 uses a generalized ice nucleation spectrum, which can have any functional form. Moreover, the maximum ice nuclei concentration that allows homogeneous freezing (used to scale N_i as a function of the IN concentration in both parameterizations) in LP2007 is a function of the vertical velocity only, whereas for BN2009 it also depends on the characteristics of the ice nucleation spectrum, the dust and BC concentrations, and the cloud formation conditions. Thus BN2009 in principle allows a greater flexibility in describing heterogeneous ice nucleation. In this work the heterogeneous ice nucleation spectrum from *Phillips et al.* [2008] is used to describe ice nucleation on soot and dust IN in the deposition, condensation and immersion modes. We have adjusted the dust surface area in the *Phillips et al.* [2008] spectrum following *Eidhammer et al.* [2010]. The scheme use Aiken mode sulfate aerosol particles larger than 0.05 μm diameter and dust in the coarse mode as potential ice nuclei as with LP2007. The sulfate size threshold has been altered from LP2007 in CAM5-BN to ensure reasonable ice number concentrations and consistent global cloud radiative forcing.

2.2. ECHAM5-HAM Description

[14] For comparison to CAM5, we also perform simulations of ice nucleation using a similar methodology with a different GCM. ECHAM5-HAM is a GCM with similar capabilities to CAM5. It has a 2-moment cloud microphysics scheme with prognostic number and mass for liquid and ice [*Lohmann et al.*, 2007] coupled to a 7 mode aerosol model (HAM) [*Stier et al.*, 2005]. Aerosol effects on ice clouds are parameterized as detailed in *Lohmann et al.* [2008] using the ice nucleation parameterization of *Kärcher and Lohmann* [2002]. If the dust number concentration exceeds 10 L^{-1} heterogeneous nucleation sets in above a critical relative humidity of 130%. Otherwise cirrus form by homogeneous nucleation. BC is treated as an immersion IN in mixed phase clouds in ECHAM-HAM.

2.3. AIE Analysis

[15] There are several different ways to analyze aerosol indirect effects. To isolate effects for ice is difficult, as aerosols can also be active as cloud condensation nuclei (CCN), and also may have direct effects (scattering radiation back to space, or absorbing it in the case of BC). So we will use several different techniques to estimate the indirect effects in the simulations. Some of the complexities are described by *Lohmann et al.* [2009].

2.3.1. RFP Methods

[16] The most straightforward method diagnoses a total aerosol effect by the Radiative Flux Perturbation (RFP) in the Top Of Atmosphere (TOA) radiative flux (R) between a simulation with present-day (year 2000) emissions of aerosol and aerosol precursors and one with pre-industrial (1850) emissions ($RFP = R_{2000} - R_{1850}$). Both runs have the same Sea Surface Temperature (SST) and Greenhouse Gas (GHG) climatology (representing the years 1980–2000). The aerosol indirect effect can also be equated with a change in cloud radiative forcing ($CF = R_{all} - R_{clr}$ for LW and SW) between two runs ($AIE = dCF_{LW} + dCF_{SW}$) where R_{clr} is the TOA flux calculated without clouds and R_{all} is the flux for all conditions. In this work we will use 'd' to indicate a change between 2000 and 1850 with the same code (within one experiment), and 'Δ' to indicate differences between different experiment pairs. To isolate the effect of ice nucleation, we can difference simulation pairs with ice nucleation linked to aerosols (e.g., CAM5-LP) and simulations in which ice nucleation is estimated only as a function of temperature (CAM5-FixedIN). The FixedIN simulation follows *Cooper* [1986] as in *Gettelman et al.* [2008]. This can be estimated with the RFP so that $AIE_{ice} = \Delta RFP = RFP_{LP} - RFP_{FixedIN}$. Since the direct scattering effects of aerosols may also change between simulations, it is necessary to factor out changes to the clear sky shortwave flux (dFSC) that may vary between pairs of simulations (ΔFSC), so that $AIE_{ice} = \Delta RFP - \Delta FSC$. AIE can also be estimated with the changes in cloud radiative forcing (CF) so $AIE_{ice} = \Delta CF = dCF_{LP} - dCF_{FixedIN}$. These 3 estimates are shown in Table 5.

2.3.2. Fixed Drop Number

[17] Another approach is to fix the liquid drop number (eliminating liquid indirect effects) and just focus on the ice phase. We have also done this in the simulations, performing several experiments with fixed drop number (Table 4, FixedDN). The AIE of ice is then dRFP = dR = $R_{2000} - R_{1850}$, minus the clear sky effect of aerosols, estimated by the change in clear sky shortwave flux (dFSC), or $AIE_{ice} = d\mathrm{RFP} - d\mathrm{FSC}$. The AIE for a fixed drop number run can also be estimated by just the change in CF between 2000 and 1850 ($AIE_{ice} = d\mathrm{CF}$).

[18] These different methods provide a spread of estimates in AIE. Fortunately, we will show that they are broadly comparable and provide a consistent set of numbers.

2.4. Experiment Description

[19] Each experiment listed in Table 1 and discussed below is two simulations, with different values of aerosol emissions representative of the years 2000 and 1850. All other inputs and boundary conditions are kept constant at year 2000 conditions (such as SST and GHGs). CAM5 simulations have horizontal resolution of 1.9° × 2.5° and are run for 6 years, analyzing the last 5 years. This is sufficient to get robust global statistics, but regional changes may not be significant. CAM5 simulations are performed using LP2007 ice nucleation (CAM5-LP), IN as fixed function of temperature (CAM5-FixedIN), BC added to LP2007 with different efficiencies (CAM5-LP-BC cases), and BN2009 ice nucleation with two different size thresholds for sulfate particles (CAM5-BN and CAM5-BN-Low). We also perform simulations with an alternative ice tuning for LP2007 (CAM5-LP-Low) that has similar global cloud forcing but 40% less ice to accommodate changes to liquid clouds. A sensitivity test was performed with sub-grid vertical velocity for ice nucleation increased by a factor of 10 (CAM5-LP-W10). We also perform fixed drop number experiments with LP2007 (CAM5-LP-FixedDN) and BN2009 (CAM5-BN-FixedDN), and with ECHAM5-HAM (ECHAM5-FixedDN). Drop number is not allowed to vary from a prescribed value set to produce reasonably present-day cloud forcing.

3. Results: Ice Nucleation

3.1. Evaluation of CAM

[20] CAM5 has been extensively evaluated for the ice phase in the upper troposphere against observations by *Gettelman et al.* [2010]. The CAM5.1 model used here performs essentially identically with respect to ice mass and ice supersaturation. The simulations for the base case are very similar to *Liu et al.* [2012b], with the exception that *Liu et al.* [2012b] increase the sulfate (SO_4) in ice nucleation by including all sulfate, while here and in *Gettelman et al.* [2010] we limit sulfate in ice nucleation to D > 0.1 μm in the CAM5-LP case. We will show a few examples of ice cloud microphysics from the simulations, and reference other work that has validated the base case climatology.

[21] Here we look briefly at the climatology of cirrus cloud microphysics in the base CAM5 (CAM5-LP) simulations. Figure 1 illustrates annual mean ice effective radius (Figures 1a and 1b) and number concentration (Figures 1c and 1d) for the upper troposphere at 2 levels. 142 hPa (Figures 1a and 1c) features tropical cirrus clouds in the Tropical Tropopause Layer (TTL), while 232 hPa (Figures 1b and 1d) also includes cirrus clouds in middle and high latitudes. For tropical cirrus at 142 hPa (Figures 1a and 1c), simulated N_i averages 110 L^{-1}(Table 2) with a range from 100–300 L^{-1}. Simulated effective radii (Figure 1a) are from 20–50 μm. At lower altitudes and warmer temperatures (232 hPa), simulated ice N_i is generally lower, 100–200 L^{-1} over land and only 50–70 L^{-1} over ocean (Figure 1d). Simulated size is larger, and peaks at 70 μm in the tropics, and 45 μm in midlatitudes. N_i in these simulations is lower than in *Liu et al.* [2012b], due to the difference in sulfate number used.

[22] To compare these simulated values to observations, Figure 2 illustrates the number concentration (Figure 2a) and (number weighted) effective radius (Figure 2b) as a function of temperature. Collected aircraft observations for tropical and midlatitude cirrus reported by *Krämer et al.* [2009, Figure 9] are also shown in Figure 2 (gray symbols) with error bars indicating 25th through 75th percentile, and 'X' indicating the median (50th percentile). Percentiles follow *Wang and Penner* [2010], and effective radii are area weighted to compare to the model (they are multiplied from what appears in *Krämer et al.* [2009] by a factor of 3 to account for difference from number weighting assuming an exponential distribution). Also shown are observations of thin tropopause level cirrus from *Lawson et al.* [2008] (black square) and tropical convective outflow cirrus from *Jensen et al.* [2009] (black triangle). Simulated values are monthly means. In most cases, the most frequently observed value is the 25th percentile (lower concentration in Figure 2a), as noted in *Salzmann et al.* [2010]. CAM5-LP (orange) N_i (Figure 2a) is slightly higher than observed at low temperatures, and lower at higher temperatures than observed. This indicates a different gradient than observations, likely due to the predominance of homogenous nucleation at lower temperatures. Some of the simulations (e.g., CAM5-BN-Low) do have N_i closer to observations (50–150 L^{-1} at 190 K). As a result, the ice effective radius (number weighted), is generally smaller than observed at low temperatures, but similar to observed at higher temperatures. Above 210 K, agreement between CAM5-LP and observations is good, with a tendency toward smaller radius and higher N_i at low temperatures. This might be due to suppression of homogenous freezing [*Jensen et al.*, 2005]. ECHAM5-HAM (red) has higher N_i and smaller sizes at warmer temperatures. The spread of simulations allows a test of the impact of these differences on the resulting ice indirect effects.

[23] As illustrated by *Gettelman et al.* [2010, Figure 10], CAM5 generates reasonable values and frequency of occurrence of ice supersaturation when compared with available in-situ aircraft or satellite observations. Maximum values of about 150% RHi are seen, which is close to the threshold for homogeneous nucleation (150–160% at the coldest temperatures). These values are similar to *Liu et al.* [2012b], but the different balance of homogeneous and heterogeneous nucleation alters some of the details at high ice supersaturation.

[24] As shown by *Liu et al.* [2012b] and *Gettelman et al.* [2010], CAM5 generally is able to reproduce important radiative properties of clouds. Cloud radiative forcing and cloud fraction compare favorably to satellite observations [*Gettelman et al.*, 2010, Figure 12; *Liu et al.*, 2012b, Figure 8], as do ice mass in the atmosphere, and the partitioning between liquid and ice phases with temperature [*Gettelman et al.*, 2010,

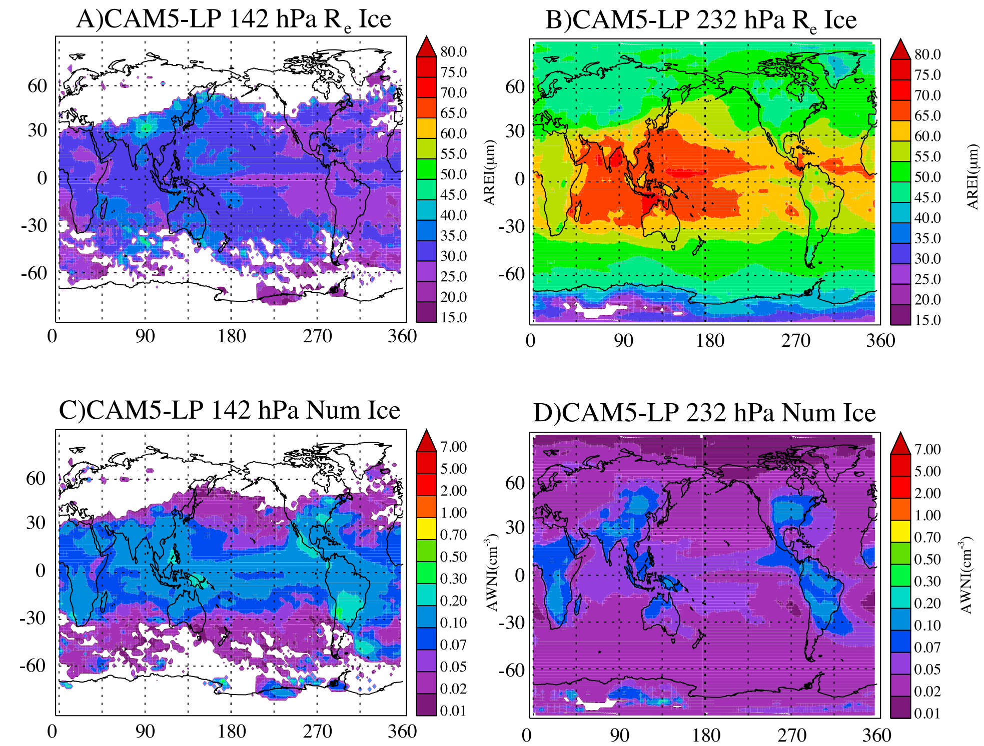

Figure 1. Maps of annual mean (a and b) simulated ice effective radius (R_e) and (c and d) ice number concentration at 232 (Figures 1b and 1d) & 142 (Figures 1a and 1c) hPa from the Base CAM5-LP simulation (year 2000).

Figure 3]. These results indicate that the simulations are capable of representing the base state of cirrus and mixed phase clouds.

[25] We performed a test to understand the sensitivity of the results to the assumed sub-grid vertical velocity used to drive ice nucleation (CAM5-LP-W10). Results indicate a near doubling of ice crystal numbers (Table 2) to values that are significantly higher than observations, and several W m^{-2} increase in the gross cloud forcing (brighter clouds).

3.2. Impact of Ice Nucleation

[26] Now we look at the changes to the simulations from different ice nucleation approaches. We first look at the change between the CAM5-FixedIN case and CAM5-LP case that incorporates the effects of aerosols. We then explore differences with the CAM5-BN case. We look also at the impact of adding BC to the ice nucleation in CAM5-LP-BC, as originally included in LP2007, but removed in CAM5 [*Gettelman et al.*, 2010] and the CAM5-LP case.

[27] Figure 3 compares the grid box averaged ice (not including snow) mass (Figures 3a and 3b) and in-cloud ice number (Figures 3c and 3d) between CAM5-LP (Figures 3a and 3c) and the ice nucleation fixed as a function of temperature following *Cooper* [1986], CAM5-FixedIN (Figures 3b and 3d). All else being equal in the simulations, the CAM5-FixedIN simulation has less ice mass and significantly lower

Table 2. Key Cloud Properties in Base Case (Year 2000 Runs)[a]

Run	SWCF (Gbl) (Wm^{-2})	LWCF (Gbl) (Wm^{-2})	IWP (Gbl) (g m^{-2})	INC150 (L^{-1})	REI150 (μm)
Observed	−47.1	26.5			
CAM5-LP	−51.8	24.0	17.7	111	31
CAM5-FixedIN	−49.2	18.5	13.1	11	41
CAM5-LP-BC 0.1%	−51.5	23.6	17.5	102	31
CAM5-LP-BC 2%	−57.8	31.5	22.3	184	27
CAM5-LP-BC 100%	−78.3	51.8	33.9	2180	20
CAM5-BN	−51.6	23.7	16.9	252	27
CAM5-LP-Low	−51.7	23.5	10.7	131	29
CAM5-BN-Low	−49.0	20.7	15.5	34	40
CAM5-LP-W10	−54.7	27.7	20.4	200	29
CAM5-LP-FixedDN	−53.7	24.1	10.8	135	28
CAM5-BN-FixedDN	−53.1	27.1	11.4	686	24
ECHAM5-FixedDN	−52.5	27.3	4.8	986	32

[a]Shown are global Short Wave Cloud Forcing (SWCF), Longwave Cloud Forcing (LWCF) and Ice Water Path (IWP). Also shown are tropical (30S–30N) averages at 150 hPa of ice effective radius (REI150) and ice number concentration (INC150). Observations of cloud forcing are from updated version 2.1 of the CERES-EBAF data described by *Loeb et al.* [2009].

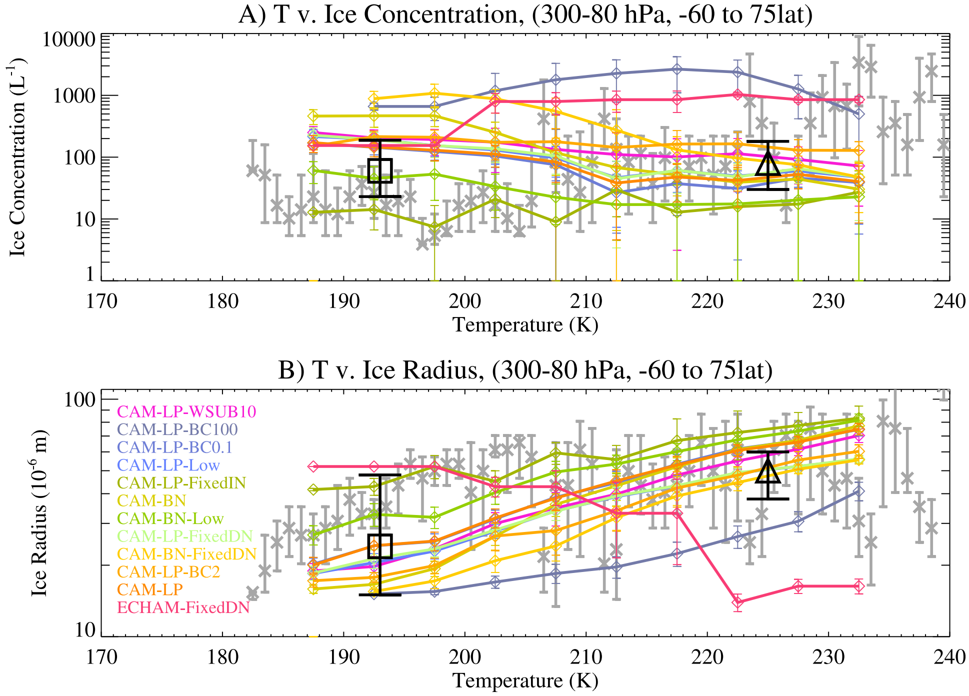

Figure 2. Annual mean simulated ice (a) number concentration (N_i) and (b) area weighted effective radius (R_e) from year 2000 simulations of different experiments (colored lines). Error bars indicate 1 standard deviation of individual points in a temperature bin. Also shown are observations from *Krämer et al.* [2009] (gray) with error bars indicating the 25th and 75th percentile range, with median (50th percentile) indicated by 'X'. Also shown are estimates in sub-visible cirrus by *Lawson et al.* [2008] (squares), and observations in tropical anvil clouds by *Jensen et al.* [2009] (triangles).

ice number in the tropical upper troposphere at cirrus altitudes (300–100 hPa). The tropical average N_i at 142 hPa in CAM5-FixedIN is one order of magnitude lower than the CAM5-LP case (Table 2). These differences are not unexpected since the CAM5-Fixed IN run has a constant activated IN concentration of 209 L^{-1} for T < $-30°C$, generally less than either CAM5-LP or CAM5-BN. There are also significant differences at high latitudes, with less ice in polar regions. In the Northern Hemisphere, the reduced ice in the CAM5-FixedIN simulation has higher liquid mass below it (not shown). In the CAM5-FixedIN case, reduced ice sedimentation and precipitation as snow collects less liquid at lower levels and allows liquid concentrations to be higher than the base case. This has significant impacts on the surface radiation budget in the Arctic (not shown).

3.3. Effect of Alternative Ice Nucleation

[28] There are also significant impacts when the BN2009 scheme is used to nucleate ice heterogeneously and homogeneously (CAM5-BN). A key feature of these simulations is that the BN2009 scheme has more active ice nucleation with higher ice numbers (2.5×) than the CAM5-LP case (Table 2). This is because the threshold diameter for sulfate aerosols has been decreased from 0.1 (CAM5-BN-Low) to 0.05 μm (CAM5-BN) to maintain the energy balance at the top of the atmosphere. With the larger size threshold (the CAM5-BN-Low case), the BN2009 scheme produces lower ice numbers (more similar to observations by *Krämer et al.* [2009, Figure 2] and has very low LW cloud forcing when compared to observations from the Clouds and the Earths Radiant Energy System (CERES) satellite [*Loeb et al.*, 2009], as illustrated in Table 2 (CAM5-BN-Low). We will examine the AIE of this low ice number case however, since at cold temperatures CAM5-BN-Low has ice numbers and sizes closer to observations (Figure 2).

[29] With the BN2009 scheme (CAM5-BN), the ice nucleation has changed substantially. Figure 4 shows the fraction of activated ice nuclei from homogeneous freezing in the CAM5-LP case (Figure 4a) and the CAM5-BN case (Figure 4b). In CAM5-LP there is a balance between homogeneous and heterogeneous nucleation. Particularly in the Northern Hemisphere, with high dust loading, there is significant heterogeneous nucleation in the upper troposphere. With the BN2009 parameterization as used in CAM5-BN, almost all ice nucleation in the upper troposphere is due to homogeneous freezing (Figure 4b). A similar result has been noted by *Liu et al.* [2012b]. The result is a climate simulation with similar radiative transfer and cloud forcing (Table 2), but a very different microphysical balance of clouds.

3.4. Impact of Black Carbon

[30] We also explore adding Black Carbon (BC) as an ice nucleus in the LP2007 scheme. This is done with three cases (CAM5-BC) at different efficiencies for BC as an efficient heterogeneous ice nucleus. Table 2 illustrates that there is a strong sensitivity to the fraction of BC that can serve as IN. Here we explore the assumption that either all (100%) or small fractions (2%, 0.1%) of BC are efficient ice nuclei, behaving like dust and nucleating heterogeneously at RH_i = 130% as in LP2007. Even with 0.1% BC, there is a

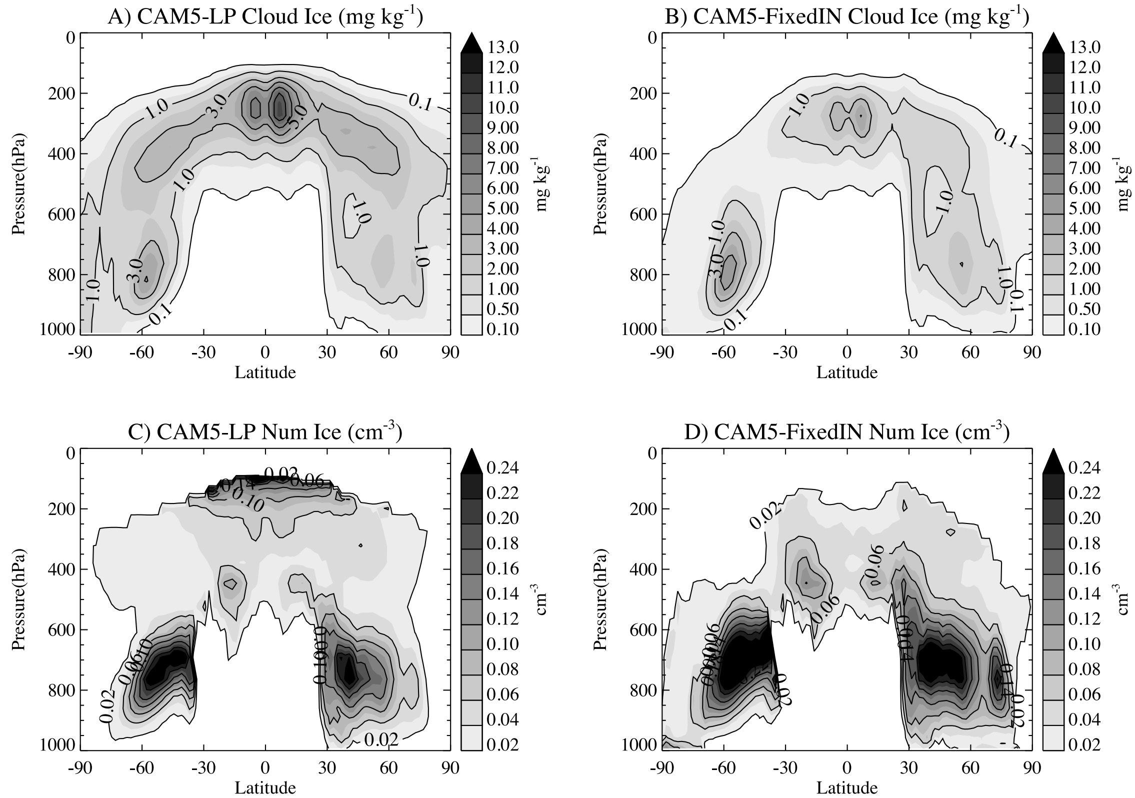

Figure 3. Zonal mean (a and b) CAM5 simulated ice mass and (c and d) number concentration from the Base (Figures 3a and 3c) and Fixed IN (Figures 3b and 3d) year 2000 simulations.

significant shift in the balance between homogeneous and heterogeneous nucleation from the base CAM5-LP case (Figure 4a) toward heterogeneous nucleation dominating, especially in the Northern Hemisphere (Figure 5a). With 2% BC available for activation, almost all ice nucleation occurs heterogeneously (Figure 5b). Table 2 indicates that for the case of 100% BC and 2% BC the gross cloud forcing is unrealistically high compared to observations from CERES observations [*Loeb et al.*, 2009] shown in Table 2 by a factor of 1.5–2 (LW and SW) for the 100% case, and 1.3–1.1 (LW and SW) for the 2% BC case, and a doubling (2%) or tripling (100%) of the ice mass, with large increases in ice number. For the 0.1% BC case (CAM5-LP-BC 0.1%), there is little impact on the simulated climate, and the energy balance of this run remains similar to observations and the CAM5-LP case. We also explored including BC ice nucleation in the BN2009 scheme (not shown). BN2009 assumes a reduced capability of BC as an IN, and also has higher homogeneous nucleation, so there was little impact seen in the simulation for adding BC as IN.

4. Results: Aerosol Indirect Effects

[31] Given this set of simulations, we now have several different model configurations with very different microphysical balances, but similar climate states. Based on the spread in current observations (Figure 2) these states are not distinguishable from each other. Even the large differences

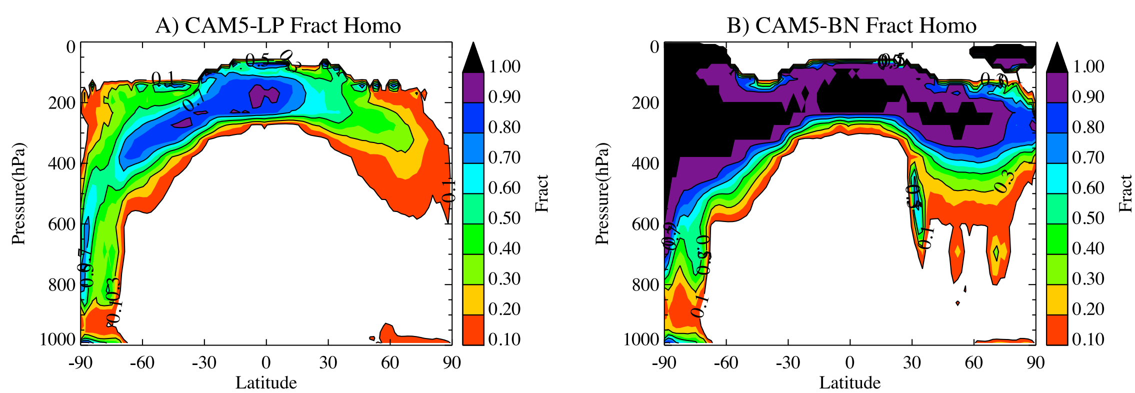

Figure 4. Zonal Mean fraction of activated IN due to homogeneous nucleation in the year 2000 (a) CAM5-LP and (b) CAM5-BN simulations.

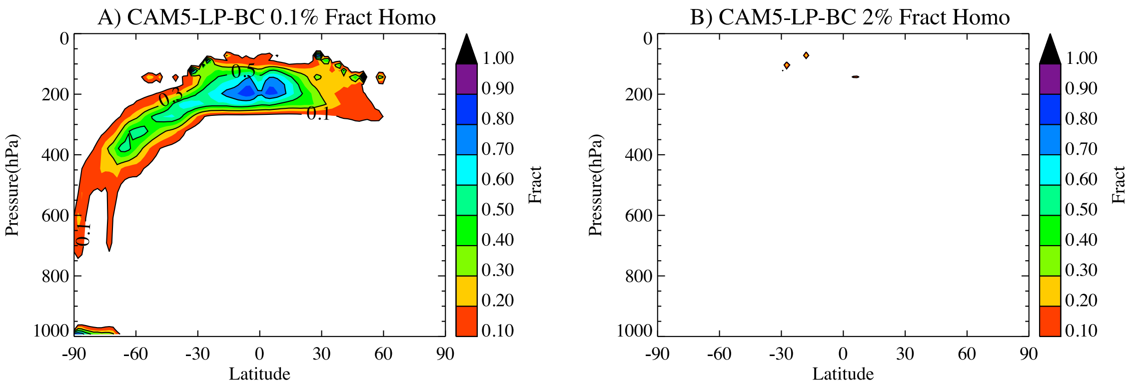

Figure 5. Zonal Mean fraction of activated IN due to homogeneous nucleation in the year 2000 CAM5-LP-BC simulations with (a) 0.1% BC and (b) 2% BC efficiencies.

between the BN and Base case ice number in the upper troposphere do not have a large impact on cloud radiative forcing (Table 2). Cloud radiative forcing is similar because the microphysical balance of clouds (ice number, habit and mass) combine in a non-unique function to generate similar radiative forcing from different states. The question remains: will these different states and different balances of ice nucleation result in differences in how ice clouds change, for example, in response to aerosol perturbations?

[32] We use the CAM5 and ECHAM5-HAM experiments to test this hypothesis. We perform an additional set of experiments where the emissions of aerosols reflect emissions in 1850. All other aspects of these simulations (GHGs and SSTs) remain the same. First we analyze the quantitative AIE of all clouds in the simulations, then discuss differences between the various simulations for ice AIE. The basic statistics of the differences between the 2000 and 1850 emission runs are shown in Table 3. The total liquid and ice AIE from the CAM5-LP case is ~ -1.0 Wm^{-2}, when estimated either from the change in cloud radiative forcing (dCF $= -1.11$ Wm^{-2}), or the change in RFP, adjusted for the direct effect of aerosol scattering (dR $-$ dFSC $= -1.36 + 0.37 = -0.99$ Wm^{-2}).

4.1. Difference From Fixed IN

[33] First we examine the effect of adding ice nucleation from the FixedIN simulation (CAM5-FixedIN) where aerosols do not affect cirrus clouds. Adding ice nucleation (CAM5-LP) reduces the change in top of atmosphere flux (dR) and change in cloud forcing (CF) from the fixed IN case by +0.2 Wm^{-2} (Table 3). The pattern of the change is illustrated in Figure 6. The impact is mostly confined to the northern hemisphere (where aerosol emissions change), and there are significant differences over the N. Pacific and over the Arctic. High variability in the Arctic reduces significance of regional changes there in these short (5 year) simulations, but high latitude Arctic changes do not contribute much to the global value. Most of the global effect is due not to a change in ice mass, but to a moderation of the change in liquid mass (Table 3). Based on budgets and process rates, Ice nucleation appears to have a 'glaciation' effect, where formation of ice at higher altitudes results in snow fall and accretion of liquid by the falling snow. This is particularly important for the Arctic and mixed phase clouds.

[34] In the base case simulation, the change of radiative forcing is due to a change in the ice nucleation regime. Figure 7 shows a map of the fraction of ice crystals nucleated by homogeneous freezing at 232 hPa from the CAM5-LP case for the year 2000 (Figure 7a) and 1850 (Figure 7b). Figure 7a corresponds to the same field as in Figure 4a. In 1850 homogeneous nucleation fractions are low in regions dominates by dust, especially over Europe, the Sahara, and Asia, extending into the N. Pacific. In 2000, many of these regions have significantly more homogeneous nucleation due to higher sulfate aerosol loading. In the TTL (140–

Table 3. Radiative Property Changes (Year 2000–1850) From Simulations[a]

Run	dR (Wm^{-2})	dCF (Wm^{-2})	dLWCF (Wm^{-2})	dSWCF (Wm^{-2})	dFSC (Wm^{-2})	dIWP (gm^{-2})	dLWP (gm^{-2})	dINC (L^{-1})	dREI (μm)
CAM5-FixedIN	−1.58	−1.33	0.64	−1.97	−0.29	0.07	4.7	0	0.1
CAM5-LP	−1.36	−1.11	0.54	−1.65	−0.37	0.05	3.1	19	−0.8
CAM5-LP-BC 0.1%	−1.37	−1.25	0.47	−1.72	−0.34	0.13	3.6	14	−1.3
CAM5-LP-BC 2%	−1.42	−1.44	2.45	−3.89	−0.29	0.88	4.8	58	−1.3
CAM5-LP-BC 100%	−1.96	−0.80	−1.71	0.91	1.60	−1.0	−0.4	−100	0.4
CAM5-BN	−1.31	−1.25	0.80	−2.05	−0.29	0.26	3.6	60	−1.5
CAM5-LP-Low	−1.25	−1.16	0.63	−1.79	−0.40	0.18	3.8	26	−1.2
CAM5-BN-Low	−1.25	−1.10	0.31	−1.41	−0.42	0.02	3.1	5	−1.6
CAM5-LP-W10	−1.02	−0.81	1.77	−2.58	−0.28	1.14	3.5	45	−1.3
CAM5-LP-FixedDN	−0.06	0.31	0.41	−0.10	−0.34	0.05	0.2	20	−0.9
CAM5-BN-FixedDN	0.10	0.19	1.16	−0.97	−0.20	0.32	0.8	131	0.0
ECHAM5-FixedDN	0.13	0.39	0.22	0.17	−0.32	0.03	0.14	133	−0.7

[a]Illustrated are change in top of atmosphere radiative fluxes (R), net cloud forcing (CF) as well as the long-wave (LWCF) and shortwave (SWCF) components, the change in clear-sky shortwave radiation (FSC), ice water path (IWP) and liquid water path (LWP). Also shown are tropical (30S–30N) averages at 150 hPa of changes in ice effective radius (REI) and ice number concentration (INC).

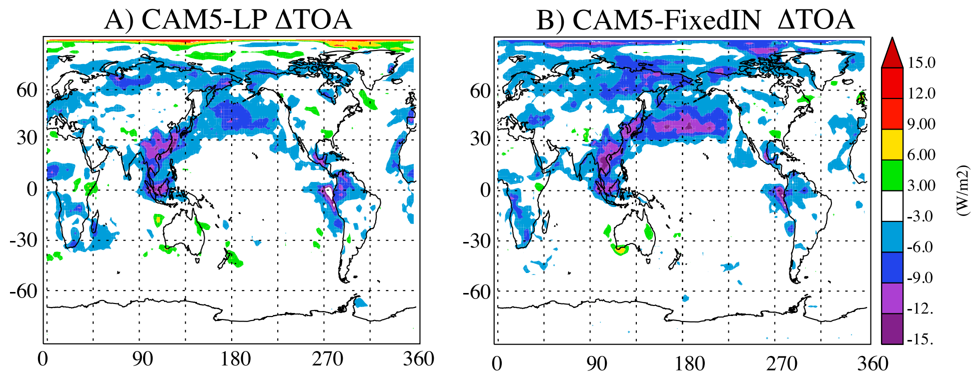

Figure 6. AIE from ice clouds estimated by change in Top of Atmosphere (TOA) radiation (dR) between 2000 and 1850 from (a) CAM5-LP and (b) CAM5-FixedIN simulations.

100 hPa) ice number increases by 20% between 1850 and 2000 (Table 3). Thus the balance of ice nucleation is shifting due mostly to increased upper tropospheric sulfate enhancing homogeneous ice nucleation. This affects ice number and radiative properties of cirrus clouds.

[35] For small nucleation efficiencies (0.1%), the effect of BC on AIE is not large (Table 3, case CAM5-LP-BC 0.1%). For higher efficiencies (CAM5-LP-BC 2% or 100%) the base state of the simulations indicates significantly higher gross cloud radiative forcing (Table 2). Analysis of these runs for AIE is hence difficult. However, the runs feature significantly more heterogeneous nucleation due to soot freezing in the immersion mode. For high soot activation, this causes a qualitative change in the effect of anthropogenic emissions. CAM5-LP-BC 100% has reductions (not increases) in crystal number, and increases in crystal size (Table 3) due to the anthropogenic effects of aerosols, changing the sign of the perturbation to the LW and SW cloud forcing. This is probably because homogeneous freezing is limited due to more efficient heterogeneous freezing on BC. However, neither the 2% or 100% case has a 'realistic' climate. The definition of 'realistic' has many dimensions, but here we illustrate it by comparison to the overall cloud radiative forcing (CF) from observations in Table 2. CF is simply a fundamental indicator of the cloud thickness and microphysics and strong gross forcing indicates clouds which differ significantly from observations (also seen in number concentrations in Table 2).

4.2. Fixed Drop Number

[36] Another way to isolate the impact of ice nucleation on clouds is to perform simulations where the liquid clouds have a fixed drop number, and droplet activation does not depend on aerosols. This eliminates any direct liquid cloud response to changing aerosol emissions (though semi-direct effects of direct aerosol heating may occur). Three simulations with fixed drop number were conducted to estimate AIE from ice clouds: CAM5 with LP2007 (CAM5-LP-FixedDN), CAM with BN2009 (CAM5-BN-FixedDN), and one with ECHAM5-HAM (ECHAM5-FixedDN). Table 3 indicates almost no change in top of atmosphere radiation in the FixedDN runs, because the SW cooling effects of aerosols in the clear sky (dFSC in Table 3) are also acting in these simulations to offset the change in cloud forcing. Hence we look at the net cloud forcing as a measure of the ice only AIE for these runs in Figure 8, using both LP and BN parameterizations. In both cases in Figure 8 the patterns are noisy due to a small signal. However, most of the signal is in the N. Hemisphere with regional perturbations of 3 Wm^{-2} or more. For the CAM5-LP-FixedDN simulations, the signal is concentrated over Europe, E. North America, E. Asia and the N. Pacific, all regions of high anthropogenic sulfate emissions. The signal in the cloud forcing is a net warming of $\sim$0.3 Wm^{-2}.

[37] The change in cloud forcing between 1850 and 2000 in a fixed drop number run has also been analyzed in ECHAM5-

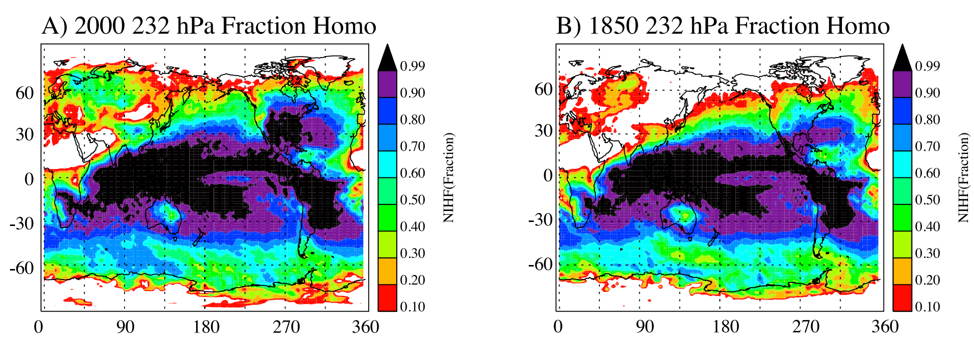

Figure 7. Map of 232 hPa fraction of ice crystals nucleated due to homogeneous freezing in the CAM5 Base simulations for (a) 2000 and (b) 1850.

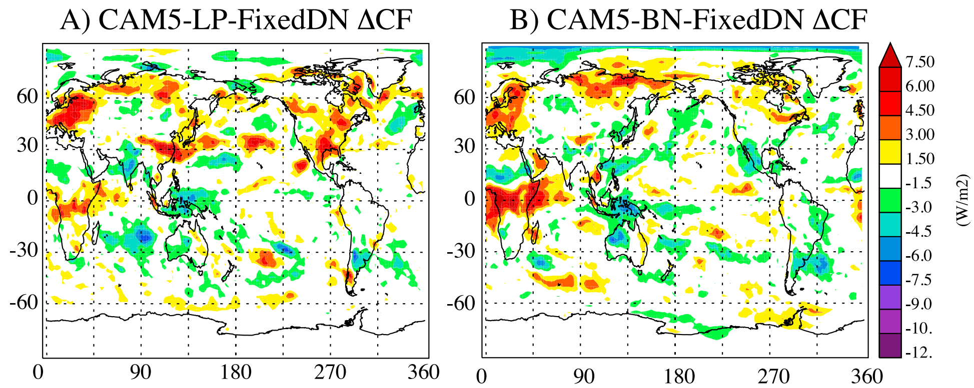

Figure 8. AIE from ice clouds estimated from the change in Cloud Forcing (ΔCF) from CAM5 fixed drop number runs between 2000 and 1850 for (a) CAM5-LP-FixedDN and (b) CAM5-BN-FixedDN.

FixedDN (Table 3). The change in cloud forcing is slightly higher than in CAM5-LP-FixedDN (0.4 Wm^{-2}, Table 3), but the mechanism is different. In ECHAM5-FixedDN, there is an increase in longwave forcing (dLWCF, Table 3) but also a decrease in shortwave forcing (positive dSWCF in Table 3), associated with higher ice crystal numbers and slightly smaller sizes (Table 3). This arises despite an increase in heterogeneous nucleation in present-day, because more dust coated by sulfate and soluble organics is available. In the LP2007 scheme (CAM5-LP, with or without BC), heterogeneous immersion freezing occurs for coarse mode dust, independent of sulfate coating. Thus a change in the heterogeneous immersion freezing of sulfate coated dust is not included in CAM5, so heterogeneous freezing of dust acts in the same way in CAM5 in 2000 and 1850. The ice water path is lower in ECHAM5-FixedDN (4.8 g m^{-2}) than in CAM5 (17.7 g m^{-2}, Table 2). An increase in ice crystal number in ECHAM5-FixedDN has a larger effect in the LW than the SW for thin clouds [*Fusina et al.*, 2007]. However, in ECHAM5-FixedDN, the cloud cover is also slightly reduced (not shown) so that the shortwave cloud forcing decreases slightly (positive dSWCF in Table 3). The longwave cloud forcing increases as the increase in ice water path with more numerous and smaller ice crystals outweighs the decrease in cloud cover. There is virtually no change in cloud cover in CAM5, so the effects are only due to cloud microphysical changes. There are thus two differences between CAM5 and ECHAM-HAM. First the treatment of BC as heterogeneous immersion freezing nuclei in ECHAM-HAM. Second, the net effect on cloud forcing in each model is the same, but for different reasons: thinner clouds are changing their LW and SW balance differently in ECHAM5-HAM than in thicker CAM clouds, combined with effects of changes in cloud area coverage in ECHAM5-HAM.

4.3. Net AIE

[38] There are several different ways to calculate the net AIE of ice clouds in the simulations, as detailed in Section 2.3. The two basic methods are to estimate it from the fixed drop number simulations, where liquid clouds do not change, or to estimate the impact as a difference from the effects in the Fixed-IN run using ice nucleation as a function of temperature. The results are generally consistent between methods. We also explore whether significant differences exist in the AIE of cirrus clouds with the different ice nucleation parameterizations and microphysical balance, or with the inclusion of Black Carbon as IN.

[39] First we estimate the ice indirect effect from the fixed drop number runs. This can be done in two ways, using either the change in cloud forcing (dCF) or the change in flux (dR) adjusted for the direct scattering effects of aerosols (dR - dFSC). Table 4 illustrates these values. For the LP2007 simulation with fixed drop number (CAM5-LP-FixedDN), both values are essentially the same (∼0.3 Wm^{-2}). There is slightly more spread in the two values from the CAM5-BN-FixedDN simulation, but they both indicate a warming due to anthropogenic aerosols of 0.2–0.3 Wm^{-2}. The gross change in cloud forcing in the BN fixed drop number case (Table 3, dLWCF and dSWCF) is significantly larger. This may be due to the dominance of homogeneous nucleation in the base case (and lack of heterogeneous nucleation). The results indicate that in both cases the increase in homogeneous nucleation increases the gross cloud forcing, but the LW dominates over the SW. There is no evidence of significantly different cirrus AIE with the different ice nucleation schemes. Results from ECHAM5-FixedDN simulations are similar, but as noted arise from a different response (increasing heterogeneous nucleation), with reductions in SW cloud forcing resulting in a similar effect.

[40] We can also look at how various CAM5 simulations differ from the CAM5-FixedIN runs. As detailed in Section 2.3, differences are denoted by 'Δ' in Table 5, and represent differences between the 2000–1850 changes ('*d*') in Table 3 between simulations and the FixedIN case. Results are presented in Table 5 using 3 different estimates. AIE estimates as a difference from the Fixed IN case differ between methods by 0.1–0.2 Wm^{-2}. This is a significant fraction of the mean value, but all estimates have the same

Table 4. Summary of AIE Estimates From Different Fixed Drop Number Runs in Wm^{-2} as the Change Between Runs With 2000 and 1850 Aerosol Emissions[a]

Run	*d*CF	*d*R -*d*FSC
CAM5-LP-FixedDN	0.31	0.28
CAM5-BN-FixedDN	0.19	0.30
ECHAM5-FixedDN	0.39	0.45

[a]Columns indicate change in cloud forcing (*d*CF) and change in TOA flux exclusive of clear-sky shortwave change due to direct effect of aerosols (*d*R -*d*FSC). See text for details. Simulations from Table 1.

Table 5. AIE as Differences (Δ) From Fixed IN Runs (in Wm^{-2})[a]

Run	ΔRFP	ΔRFP - ΔFSC	ΔCF	Mean
CAM5-LP	0.22	0.30	0.22	0.25
CAM5-LP-BC 0.1%	0.22	0.27	0.08	0.19
CAM5-BN	0.27	0.27	0.08	0.21
CAM5-LP-Low	0.33	0.44	0.17	0.31
CAM5-BN-Low	0.33	0.46	0.23	0.34
CAM5-LP-W10	0.56	0.55	0.52	0.53
CAM5-LP-BC 2%	0.16	0.17	−0.11	0.08

[a]Columns indicate change in TOA flux (R) (or the RFP) between two runs (ΔRFP), the change in RFP exclusive of the clear-sky shortwave change due to direct effect of aerosols (ΔRFP - ΔFSC), the change in cloud forcing (ΔCF) and the mean of these three estimates. See text for details. Simulations from Table 1. The last 2 simulations (W10 and BC 2%) are sensitivity tests that are not included in the average values reported since their basic states are very different.

sign (positive) and similar magnitude. There is not much systematic difference in the ice AIE diagnosed from the different simulations. The CAM5-LP-Low case, with lower ice mass appears to be slightly more sensitive to changes in IN (mean AIE of 0.31 Wm^{-2}) than the CAM5-LP case (mean AIE of 0.25 Wm^{-2}). The fixed drop number simulations are performed with the CAM5-LP-Low microphysical balance, and so these estimates are consistent with the fixed drop number estimates above. The CAM5-BN case has a slightly lower average AIE (0.21 Wm^{-2}), probably because of the larger fraction of homogeneous nucleation and less heterogeneous nucleation makes it less sensitive while the CAM5-BN-Low case has much lower ice number concentrations (Table 2), more similar to observations at cold temperatures (Figure 2). This simulation with lower ice number concentrations has a relatively large change in ice number concentration due to present-day aerosol emissions (Table 3), and consequently a slightly larger ice AIE (Table 5), of 0.23–0.46 W m^{-2} depending on method used to estimate it.

[41] Because the ice nucleation parameterizations are sensitive to vertical velocity, we also perform a sensitivity test to understand the impact of different assumptions on ice AIE. The CAM5-LP-W10 simulation has vertical velocities which are generally higher than those observed in cirrus clouds (>0.5 ms^{-1}). With significantly higher sub-grid vertical velocities (CAM5-LP-W10) N_i is higher (Table 2). Cloud forcing is strong (Table 2) and the resulting ice AIE is stronger (∼0.5 Wm^{-2}, Table 5). This case is an extreme, and illustrates moderate sensitivity to sub-grid vertical velocity, but not enough to alter the general conclusions of the paper.

[42] Finally we consider the impact of BC on AIE for cirrus clouds. To do so, we look at the differences between the estimates of AIE derived using variations from the Fixed IN runs in Table 5. For the higher efficiency BC cases (CAM5-LP-BC 2% and 100%), the mean state is significantly different from the CAM5-Fixed IN case, so we do not analyze the ice AIE quantitatively as a difference from the CAM5-Fixed IN run. The mean of three estimates from the CAM5-LP case is 0.25 Wm^{-2}, while that of the CAM5-LP-BC 0.1% case is 0.19 Wm^{-2}. The increase in ice number with anthropogenic emissions in CAM5-LP of 19 L^{-1} (Table 3) is slightly reduced in CAM5-LP-BC 0.1% (14 L^{-1}) due to slightly more active heterogeneous BC nuclei. The difference in AIE (−0.06 Wm^{-2}) is not significant given the spread of the different estimates (standard deviation of all estimates is 0.10 Wm^{-2}). This is the impact of anthropogenic BC in ice nucleation, given an assumed efficiency in the LP2007 scheme that maintains a reasonable climate. For the CAM5-LP-BC 2% case, the same calculation yields a BC effect of −0.17 W m^{-2}. The impact of BC is of the same sign but lower than estimated by *Penner et al.* [2009] with an off-line model, likely due to lower efficiency for BC assumed here.

5. Discussion

[43] The simulations provide several different methods of looking at the effects of ice nucleation in the current climate, and the anthropogenic perturbation to the climate. The implementation of the LP2007 and BN2009 scheme in CAM5 performed here yield very different results for the microphysical balance of clouds. Comparison to in-situ observations of ice crystal number and size indicates that most of the simulations have slightly higher ice numbers at low temperatures. This appears to be due to the influence of homogeneous freezing at cold temperatures. We have also examined perturbations to the ice nucleation scheme that result in very different numbers and sizes, by altering the aerosol sizes used in nucleation (CAM5-BN-Low), the overall ice mass (CAM5-LP-Low), or the sub-grid vertical velocity (CAM5-LP-W10).

[44] The parameterizations are constrained with the restriction that the cloud radiative forcing be similar to observations (Section 3). Given this constraint, the BN2009 scheme (CAM5-BN) has higher ice numbers and a dominance of homogeneous nucleation over heterogeneous nucleation. Two different versions of CAM5 with the LP2007 scheme were analyzed (CAM5-LP and CAM5-LP-Low), and an alternative version with significantly less ice mass (CAM5-LP-Low) also has a significant heterogeneous nucleation fraction. The balance of homogeneous and heterogeneous nucleation is different in ECHAM5-HAM, with much lower ice water path. The simulations with lower present-day ice water path (ECHAM5-FixedDN, CAM5-LP-Low, Table 2) or low ice number (CAM5-BN-Low) appear to have slightly higher ice AIE (Tables 4 and 5). This indicates that lower mass or number implies higher sensitivity to changes.

[45] We have also investigated the impact of Black Carbon aerosols on ice nucleation in CAM5 (CAM5-LP-BC). Results depend entirely on the assumed efficiency of BC as an ice nucleus. This is highly uncertain, but most studies show little potential for significant heterogeneous nucleation on significant fractions of BC aerosols below the homogeneous nucleation limit. This study looked at the impact of assuming that different fractions of the BC number were efficient heterogeneous ice nuclei. For values of 0.1%, there is a small cooling due to reduced increase in N_i, consistent with other work [*Penner et al.*, 2009]. For higher BC efficiency (2% or 100%) gross cloud forcing was significantly larger than observations (Table 2). Thus a high efficiency is not consistent with the CAM5 formulations used here. The BC treatment using BN2009 did not impact climate or ice cloud microphysics significantly (not shown).

[46] In all CAM5 cases examined, the ice nucleation balance shifts to more homogeneous nucleation as sulfate increases from pre-industrial (1850) to present (2000). *Seifert et al.* [2004] found using in-situ data that increases in (sulfate)

aerosol number density corresponded to increased ice number concentrations. The effect is complex, however this lends observational support that an increase in ice crystal number from increased sulfate is plausible. The opposite effect was noted in ECHAM5-HAM (see below).

[47] Using the sensitivity tests as a measure of the uncertainty, we can summarize the ice AIE results. If all experiments, models and estimates are treated equally from Tables 4 and 5 this yields 21 estimates from simulations with reasonable basic states with a mean of 0.27 ± 0.10 Wm^{-2}, where the uncertainty is one standard deviation. The CAM5-LP-W10, CAM5-LP-BC 2% and CAM5-LP-BC 100% experiments are not included in this estimate, since their basic states are quite different than observations, or other simulations. The estimate represents about 20% of the total simulated change in shortwave cloud forcing (shortwave AIE) for liquid and ice clouds in CAM5 of -1.6 Wm^{-2}, and is of the opposite sign. The indirect effect of cirrus in CAM5 simulations is to drive clouds toward increased homogeneous nucleation, 20% higher ice number concentration, and an increase in gross cirrus cloud radiative forcing, with the long-wave slightly larger than the shortwave effect, resulting in a warming. The CAM5 experiments with more heterogeneous nucleation (CAM5-LP-Low) are more sensitive to changing emissions, and have slightly higher AIE than the base (CAM5-LP) case, or the CAM5-BN case with mostly homogeneous nucleation. The effect of adding BC as heterogeneous nuclei slightly reduces the warming (-0.06 Wm^{-2}), but not significantly.

[48] The ECHAM5-HAM results indicate similar AIE but for different reasons. In this simulation the ice clouds are thinner, with significantly less ice, and the change from pre-industrial to present-day is an increase in heterogeneous nucleation due to dust coated with sulfate and soluble organics, while CAM5 has an increase in homogeneous freezing due to sulfate. An increase in heterogeneous freezing can lead to more or less ice crystals depending on updraft velocity [*Kärcher and Lohmann*, 2003]. In these ECHAM5-HAM simulations heterogeneous freezing causes an increase in ice crystal number. This nevertheless results in a smaller shortwave cloud forcing because the cloud cover decreases. This adds to the longwave warming. Thus the increase in crystal number makes the LW positive and SW negative, but the change in cloud cover has the opposite effect. The combination for the thin ECHAM5-HAM clouds (low IWP) is positive. That the overall results are similar between CAM5-FixedDN and ECHAM5-FixedDN is function of the different ice water path in the ECHAM5-FixedDN and CAM5-FixedDN simulations and the ECHAM5-FixedDN cloud cover change.

[49] These simulations do not provide complete representation of all ice nucleation mechanisms. Soluble organics have been found to be IN when they become solid at very cold temperatures [*Murray et al.*, 2010], which might help explain low ice crystal numbers and impede ice crystal formation [*Zobrist et al.*, 2008]. There are also suggestions that oxalic acid [*Zobrist et al.*, 2006] or crystalline ammonium sulfate [*Abbatt et al.*, 2006] could act as heterogenous IN, reducing ice crystal numbers. *Hendricks et al.* [2011] and *Wang et al.* [2010] also found that including BC and other heterogenous ice nuclei reduced N_i. Note that our increases in ice crystal numbers are occurring with the increase in sulfate from pre-industrial to present-day. Simulations with more heterogenous nucleation (e.g, CAM5-LP or preindustrial cases) tend to have lower ice crystal numbers, consistent with *Hendricks et al.* [2011]. We have examined simulations with a wide base state of ice clouds, with varying balances of heterogeneous and homogenous nucleation (and ice number concentrations), and found consistent results even with different mechanisms, lending some confidence that 'missing' present-day IN that altered (lowered) simulated N_i would not significantly alter the results that depend on changing sulfate and a more consistent shift toward increased crystal number due to homogeneous freezing (CAM5) or heterogeneous freezing (ECHAM5-HAM).

6. Conclusions

[50] This work uses 2 GCMs with ice supersaturation and ice nucleation, and 3 commonly used ice nucleation schemes in large scale models. The GCM simulations generally are on the high end of observations of ice crystal number concentration at low (tropical cirrus) temperatures. Several sensitivity tests have lower ice concentrations consistent with observations, but the ice AIE results are similar. Different ice microphysical states occur with different parameterizations of the ice cloud nucleation process. At reasonable BC nucleation efficiencies (0.1%) that are consistent with laboratory measurements, BC reduces N_i and cools slightly. High BC efficiencies are not consistent with observed global radiative balance of clouds in CAM5-LP. In CAM, indirect effects of cirrus clouds occur mostly due to increases in ice crystal concentrations due to homogeneous nucleation from anthropogenic sulfur emissions. The resulting ice indirect effects are slightly larger for those states with less homogeneous nucleation and smaller ice numbers. There is a moderate sensitivity to sub-grid vertical velocities assumed for ice (higher ice AIE with higher sub-grid velocity and larger N_i). In simulations with low ice numbers (CAM5-BN-Low), ice AIE is 20–50% larger, suggesting that low ice number states may be more sensitive to perturbations.

[51] The ECHAM model has similar ice AIE, but for different reasons. In ECHAM5-HAM, thinner ice clouds and the treatment of immersion freezing of mineral dust result in an increase in heterogeneous nucleation and higher crystal numbers in present-day because heterogeneous freezing occurs at lower ice supersaturations and increased sulfate acts to coat dust. In ECHAM5-HAM with thin ice clouds (but high crystal numbers) the increase in crystal number is outweighed by a decrease in cloud coverage causing a reduction in SW cloud forcing (net warming). CAM5 can reproduce the positive SW cloud forcing effect for the 100% BC case (Table 3) where cloud fraction also decreases by over 1%. The mechanisms between the two models are different as a consequence of different IN parameterizations, but their effect is the same due to different mean states (ice water paths) of cirrus clouds.

[52] The total ice AIE is estimated at 0.27 ± 0.10 Wm^{-2} (1σ uncertainty). This represents about 20% of the simulated shortwave Aerosol Indirect Effects of -1.6 Wm^{-2} for CAM5-LP. We note that the simulations neglect possible effects of aerosols on convective clouds [e.g., *Lohmann*, 2008] that might alter detrained ice crystals.

[53] This work highlights that ice indirect effects are dependent on the assumed mechanisms for ice nucleation and the base state of ice clouds. Regardless of ice microphysical balance, addition of anthropogenic emissions, largely of sulfate, acts to increase ice number and results in positive forcing of consistent magnitude. To better constrain AIE on cirrus clouds, better understanding of the role of soot and sulfate in heterogeneous and homogeneous nucleation is necessary. In addition, better observations of the mean state of cirrus cloud microphysics, including ice water path and crystal size and number, would help discriminate between these realizations in CAM5 and ECHAM5-HAM and better constrain the AIE of cirrus clouds.

[54] **Acknowledgments:.** Computing resources were provided by the Climate Simulation Laboratory at National Center for Atmospheric Research (NCAR) Computational and Information Systems Laboratory. NCAR is sponsored by the U.S. National Science Foundation. This work was supported at NCAR by the Aviation Climate Change Research Initiative (ACCRI) contract DTRT57-10-C-10012 and the NASA Modeling Analysis and Prediction program, award NNX09AJ05G. D. Barahona was supported by the NASA Modeling, Analysis and Prediction program under WBS 802678.02.17.01.07. X. Liu acknowledges support of the US NSF/DOE/USDA Decadal and Regional Climate Prediction using Earth System Models (EaSM) program. The Pacific Northwest National Laboratory is operated for the US DOE by the Batelle Memorial Institute under contract DE-AC06-76RLO 1830. We thank S. T. Massie and C. Bardeen for comments, and M. Wang and K. Zhang for making available ice crystal observations.

References

Abbatt, J. P. D., S. Benz, D. J. Cziczo, Z. Kanji, U. Lohmann, and O. Möhler (2006), Solid ammonium sulfate aerosols as ice nuclei: A pathway for cirrus cloud formation, *Science*, *313*(5794), 1770–1773, doi:10.1126/science.1129726.

Barahona, D. (2011), On the ice nucleation spectrum, *Atmos. Chem. Phys. Discuss.*, *11*, 9549–9561, doi:10.5194/acp-11-9549-2011.

Barahona, D., and A. Nenes (2008), Parameterization of cirrus cloud formation in large-scale models: Homogeneous nucleation, *J. Geophys. Res.*, *113*, D11211, doi:10.1029/2007JD009355.

Barahona, D., and A. Nenes (2009), Parameterizing the competition between homogeneous and heterogenous freezing in ice cloud formation–polydisperse ice nuclei, *Atmos. Chem. Phys.*, *9*, 5933–5948.

Barahona, D., J. Rodriguez, and A. Nenes (2010), Sensitivity of the global distribution of cirrus ice crystal concentration to heterogeneous freezing, *J. Geophys. Res.*, *115*, D23213, doi:10.1029/2010JD014273.

Bigg, E. K. (1953), The formation of atmospheric ice crystals by the freezing of droplets, *Q. J. R. Meteorol. Soc.*, *79*, 510–519.

Cooper, W. A. (1986), Ice initiation in natural clouds. Precipitation enhancement—A scientific challenge, *Meteorol. Monogr.*, *43*, 29–32.

Corti, T., B. P. Luo, T. Peter, Q. Fu, and H. Vömel (2005), Mean radiative energy balance and vertical mass fluxes in the equatorial upper troposphere and lower stratosphere, *Geophys. Res. Lett.*, *32*, L06802, doi:10.1029/2004GL021889.

Crawford, I., et al. (2011), Studies of propane flame soot acting as heterogeneous ice nuclei in conjunction with single particle soot photometer measurements, *Atmos. Chem. Phys.*, *11*, 9549–9561, doi:10.5194/acp-11-9549-2011.

DeMott, P. J., M. D. Peters, A. J. Prenni, C. M. Carrico, S. M. Kreidenweis, J. L. Collett Jr., and H. Moosmüller (2009), Ice nucleation behavior of biomass combustion particles at cirrus temperatures, *J. Geophys. Res.*, *114*, D16205, doi:10.1029/2009JD012036.

DeMott, P. J., et al. (2011), Resurgence in ice nuclei measurement research, *Bull. Am. Meteorol. Soc.*, *92*, 1623–1635, doi:10.1175/2011BAMS3119.1.

Eidhammer, T., et al. (2010), Ice initiation by aerosol particles: Measured and predicted ice nuclei concentrations versus measured ice concentrations in an orographic wave cloud, *J. Atmos. Sci.*, *67*, 2417–2436, doi:10.1175/2010JAS3266.1.

Friedman, B., G. Kulkarni, J. Beranek, A. Zelenyul, J. A. Thorton, and D. J. Cziczo (2011), Ice nucleation and droplet formation by bare and coated soot particles, *J. Geophys. Res.*, *116*, D17203, doi:10.1029/2011JD015999.

Fusina, F., P. Spichtinger, and U. Lohmann (2007), Impact of ice supersaturation regions and thin cirrus on radiation in the midlatitudes, *J. Geophys. Res.*, *112*, D24S14, doi:10.1029/2007JD008449.

Gettelman, A., H. Morrison, and S. J. Ghan (2008), A new two-moment bulk stratiform cloud microphysics scheme in the NCAR Community Atmosphere Model (CAM3), Part II: Single-column and global results, *J. Clim.*, *21*(15), 3660–3679.

Gettelman, A., et al. (2010), Global simulations of ice nucleation and ice supersaturation with an improved cloud scheme in the community atmosphere model, *J. Geophys. Res.*, *115*, D18216, doi:10.1029/2009JD013797.

Hendricks, H., B. Kärcher, U. Lohmann, and M. Ponater (2005), Do aircraft black carbon emissions affect cirrus clouds on the global scale?, *Geophys. Res. Lett.*, *32*, L12814, doi:10.1029/2005GL022740.

Hendricks, J., B. Kärcher, and U. Lohmann (2011), Effects of ice nuclei on cirrus clouds in a global climate model, *J. Geophys. Res.*, *116*, D18206, doi:10.1029/2010JD015302.

Jensen, E., et al. (2005), Ice supersaturations exceeding 100% at the cold tropical tropopause: Implications for cirrus formation and dehydration, *Atmos. Chem. Phys.*, *5*, 851–862.

Jensen, E. J., et al. (2009), On the importance of small ice crystals in tropical anvil cirrus, *Atmos. Chem. Phys.*, *9*(15), 5519–5537.

Kärcher, B., and U. Lohmann (2002), A parameterization of cirrus cloud formation: Homogeneous freezing including effects of aerosol size, *J. Geophys. Res.*, *107*(D23), 4698, doi:10.1029/2001JD001429.

Kärcher, B., and U. Lohmann (2003), A parameterization of cirrus cloud formation: Heterogeneous freezing, *J. Geophys. Res.*, *108*(D14), 4402, doi:10.1029/2002JD003220.

Kärcher, B., J. Hendricks, and U. Lohmann (2006), Physically based parameterization of cirrus cloud formation for use in atmospheric models, *J. Geophys. Res.*, *111*, D01205, doi:10.1029/2005JD006219.

Kärcher, B., O. Möhler, P. J. DeMott, S. Pechtl, and F. Yu (2007), Insights into the role of soot aerosols in cirrus cloud formation, *Atmos. Chem. Phys.*, *7*, 4203–4227.

Krämer, M., et al. (2009), Ice supersaturations and cirrus cloud crystal numbers, *Atmos. Chem. Phys.*, *9*, 3505–3522.

Lawson, R. P., B. Pilson, B. Barker, Q. Mo, E. Jensen, L. Pfister, and P. Bui (2008), Aircraft measurements of microphysical properties of subvisible cirrus in the tropical tropopause layer, *Atmos. Chem. Phys.*, *8*, 1609–1620.

Liu, X., and J. E. Penner (2005), Ice nucleation parameterization for global models, *Meteorol. Z.*, *14*, 499–514.

Liu, X., J. E. Penner, S. J. Ghan, and M. Wang (2007), Inclusion of ice microphysics in the NCAR Community Atmosphere Model version 3 (CAM3), *J. Clim.*, *20*, 4526–4547.

Liu, X., J. E. Penner, and M. Wang (2009), Influence of anthropogenic sulfate and black carbon on upper tropospheric clouds in the NCAR CAM3 model coupled to the IMPACT global aerosol model, *J. Geophys. Res.*, *114*, D03204, 10.1029/2008JD010492.

Liu, X., et al. (2012a), Towards a minimal representation of aerosol direct and indirect effects: Model description and evaluation, *Geosci. Model Dev.*, *5*, 709–735, doi:10.5194/gmd-4-709-2012.

Liu, X., X. Shi, K. Zhang, E. J. Jensen, A. Gettelman, D. Barahona, A. Nenes, and P. Lawson (2012b), Sensitivity studies of dust ice nuclei effect on cirrus clouds with the Community Atmosphere Model CAM5, *Atmos. Chem. Phys. Discuss.*, *12*, 13,119–13,160, doi:10.5194/acpd-12-13119-2012.

Loeb, N. G., B. A. Wielicki, D. R. Doelling, G. L. Smith, D. F. Keyes, S. Kato, N. M. Smith, and T. Wong (2009), Towards optimal closure of the Earth's top-of-atmosphere radiation budget, *J. Clim.*, *22*, 748–766, doi:10.1175/2008JCLI2637.1.

Lohmann, U. (2008), Global anthropogenic aerosol effects on convective clouds in ECHAM5-HAM, *Atmos. Chem. Phys.*, *8*, 2115–2131.

Lohmann, U., and J. Feichter (2005), Global indirect aerosol effects: A review, *Atmos. Chem. Phys.*, *5*, 715–737.

Lohmann, U., and C. Hoose (2009), Sensitivity studies of different aerosol indirect effects in mixed-phase clouds, *Atmos. Chem. Phys.*, *9*, 8917–8934.

Lohmann, U., B. Kärcher, and J. Hendricks (2004), Sensitivity studies of cirrus clouds formed by heterogeneous freezing in the ECHAM GCM, *J. Geophys. Res.*, *109*, D16204, doi:10.1029/2003JD004443.

Lohmann, U., P. Stier, C. Hoose, S. Ferrachat, E. Roeckner, and J. Zhang (2007), Cloud microphysics and aerosol indirect effects in the global climate model ECHAM5-HAM, *Atmos. Chem. Phys.*, *7*(2), 3245–3446.

Lohmann, U., P. Spichtinger, S. Jess, T. Peter, and H. Smit (2008), Cirrus cloud formation and ice supersaturated regions in a global climate model, *Environ. Res. Lett.*, *3*(4), 045022, doi:10.1088/1748-9326/3/4/045022.

Lohmann, U., L. Rotstayn, T. Storelvmo, A. Jones, S. Menon, J. Quaas, A. Ekman, D. Koch, and R. Ruedy (2009), Total aerosol effect: Radiative forcing or radiative flux perturbation?, *Atmos. Chem. Phys. Discuss.*, *9*, 25,633–25,661.

Meyers, M. P., P. J. DeMott, and W. R. Cotton (1992), New primary ice-nucleation parameterizations in an explicit cloud model, *J. Appl. Meteorol.*, *31*, 708–721.
Möhler, O., et al. (2005), Effect of sulfuric acid coating on heterogenous ice nucleation by aerosol soot particles, *J. Geophys. Res.*, *110*, D11210, doi:10.1029/2004JD005169.
Morrison, H., J. A. Curry, and V. I. Khvorostyanov (2005), A new double-moment microphysics parameterization for application in cloud and climate models. Part I: Description, *J. Atmos. Sci.*, *62*, 1665–1677.
Murray, B. J., et al. (2010), Heterogeneous nucleation of ice particles on glassy aerosols under cirrus conditions, *Nat. Geosci.*, *3*, 233–237, doi:10.1038/NGEO817.
Neale, R. B., et al. (2010), Description of the NCAR Community Atmosphere Model (CAM5.0), *Tech. Rep. NCAR/TN-486+STR*, Natl. Cent. for Atmos. Res., Boulder, Colo.
Park, S., and C. S. Bretherton (2009), The University of Washington shallow convection and moist turbulence schemes and their impact on climate simulations with the Community Atmosphere Model, *J. Clim.*, *22*, 3449–3469.
Penner, J. E., Y. Chen, M. Wang, and X. Liu (2009), Possible influence of anthropogenic aerosols on cirrus clouds and anthropogenic forcing, *Atmos. Chem. Phys.*, *9*, 879–896.
Phillips, V. T. J., P. J. DeMott, and C. Andronache (2008), An empirical parameterization of heterogenous ice nucleation for multiple chemical species of aerosol, *J. Atmos. Sci.*, *65*, 2757–2783, doi:10.1175/2007JAS2546.1.
Pruppacher, H. R., and J. D. Klett (1997), *Microphysics of Clouds and Precipitation*, 2nd ed., Kluwer Acad., Norwell, Mass.
Salzmann, M., Y. Ming, J.-C. Golaz, P. A. Ginoux, H. Morrison, A. Gettelman, M. Krämer, and L. J. Donner (2010), Two-moment bulk stratiform cloud microphysics in the GFDL AM3 GCM: Description, evaluation, and sensitivity tests, *Atmos. Chem. Phys.*, *10*(16), 8037–8064, doi:10.5194/acp-10-8037-2010.
Seifert, M., et al. (2004), Aerosol-cirrus interactions: A number based phenomenon at all?, *Atmos. Chem. Phys.*, *4*, 293–305.
Stier, P., et al. (2005), The aerosol-climate model ECHAM5-HAM, *Atmos. Chem. Phys.*, *5*, 1125–1156.
Twomey, S. (1977), The influence of pollution on the shortwave albedo of clouds, *J. Atmos. Sci.*, *34*(7), 1149–1152.
Wang, M., and J. E. Penner (2010), Cirrus clouds in a global climate model with a statistical cirrus cloud scheme, *Atmos. Chem. Phys.*, *10*(12), 5449–5474, doi:10.5194/acp-10-5449-2010.
Wang, M., J. E. Penner, and X. Liu (2009), Coupled IMPACT aerosol and NCAR CAM3 model: Evaluation of predicted aerosol number and size distribution, *J. Geophys. Res.*, *114*, D06302, doi:10.1029/2008JD010459.
Wang, M., et al. (2010), The multi-scale aerosol-climate model PNNL-MMF: Model description and evaluation, *Geosci. Model Dev. Discuss.*, *3*(4), 1625–1695, doi:10.5194/gmdd-3-1625-2010.
Young, K. C. (1974), The role of contact nucleation in ice phase initiation of clouds, *J. Atmos. Sci.*, *31*, 768–776.
Zobrist, B., et al. (2006), Oxalic acid as a heterogeneous ice nucleus in the upper troposphere and its indirect aerosol effect, *Atmos. Chem. Phys.*, *6*(10), 3115–3129, doi:10.5194/acp-6-3115-2006.
Zobrist, B., C. Marcolli, D. A. Pedernera, and T. Koop (2008), Do atmospheric aerosols form glasses?, *Atmos. Chem. Phys.*, *8*(17), 5221–5244, doi:10.5194/acp-8-5221-2008.